PAPER

Flexible and mechanically stable antireflective coatings from nanoporous organically modified silica colloids†

Hulya Budunoglu,[ab] Adem Yildirim[ab] and Mehmet Bayindir*[abc]

We report the preparation of flexible and mechanically stable antireflective organically modified silica (ormosil) coatings at ambient conditions. Thin films are obtained from colloidal suspensions of ormosil gels which are prepared using methyltrimethoxysilane (MTMS) and tetraethyl orthosilicate (TEOS) monomers. The ormosil suspensions are directly applicable and suitable for the large-area deposition of nanoporous ormosil thin films. The nanoporosity of the films can be tuned by changing the monomer ratio of the starting solution. Thin films on flexible substrates retain their antireflective properties even after 100 cycles of excessive bending without a significant change in transmission. Furthermore, the films remained intact after water dripping and adhesive tape tests. In addition, thin films on glass substrates are found to exhibit antifogging properties after annealing at 600 °C for 30 min. The ease of fabrication and multifunctionality of these films make them ideal coatings for flexible electronic and optoelectronic devices, sensors, and solar cells.

Introduction

Antireflective (AR) coatings are required to improve the light transmission in a wide variety of applications such as solar cells, display screens, optical filters, windows and eye-wear glasses.[1,2,3] The principle of AR coatings is based on the elimination of the destructive interference between the air-coating and the coating–substrate interfaces. For an ideal AR surface the refractive index of the coating should satisfy the Fresnel equation, $n_c = (n_a n_s)^{1/2}$ where n_a and n_s are the refractive indices of air and the substrate, respectively. In addition, the thickness of the coating should be equal to $\lambda/4$, where λ is the wavelength of the incident light.[4] When glass is used as substrate ($n_s = 1.48$), n_c should be around 1.22, but homogeneous materials with such low refractive indices do not exist. In order to obtain such low effective refractive indices, air must be introduced into the film as a second phase by generating pores.[1] Also, the pores of the coating must be small enough to prevent the scattering of incident light. For example, the pores of AR coatings which are designed for visible wavelengths must be smaller than 50 nm.[5] Nanoporous thin films with AR properties have been prepared *via* many successful approaches, including sol–gel methods,[6,7,8] preparation of nanoparticle films,[9,10,11] chemical vapor deposition,[12] layer by layer deposition,[1,13] phase separation in polymer films,[14,15] and plasma etching.[16] However, most of the coatings have been deposited on rigid substrates like glass, silicon or PMMA, and the preparation of AR coatings on flexible substrates is still rare.[9,17]

Flexible AR coatings would be highly desirable for low cost electronic and photovoltaic devices and contact lenses. AR coatings on flexible substrates must successfully operate during and after many deformation steps. Also, they must be deposited on surfaces under mild conditions since plastic substrates are sensitive to high temperatures and many solvents.[18] Here, we report a facile method to prepare flexible AR thin films at ambient conditions from organically modified silica (ormosil) colloids. To prepare the ormosil colloids, we first synthesized ormosil gels by using methyltrimethoxysilane (MTMS) and tetraethyl orthosilicate (TEOS) as precursors. It is well known that the polymerization of MTMS generally results in phase separation due to the low solubility of the cyclic and cage-like structures formed during polymerization.[19,20,21] We previously prepared flexible ormosil coatings using such phase separated gels. Thanks to the phase separation, the coatings intrinsically have nanometer and micrometer sized pores which provide superhydrophobicity with extremely high water contact angles (up to 179°) and low sliding angles (<1°).[22,23] However, micrometer sized pores scatter light and result in a slightly translucent appearance. So, in order to prepare AR and flexible thin films, phase separation during gelation must be prevented. One strategy to prevent phase separation is to use an additional monomer which does not contain organic groups.[24] In this work we used TEOS as an additional monomer and we prepared homogenous ormosil gels. The homogeneous ormosil gels are

aUNAM-National Nanotechnology Research Center, Bilkent University, 06800 Ankara, Turkey
bInstitute of Materials Science and Nanotechnology, Bilkent University, 06800 Ankara, Turkey
cDepartment of Physics, Bilkent University, 06800 Ankara, Turkey. E-mail: bayindir@nano.org.tr

† Electronic supplementary information (ESI) available. See DOI: 10.1039/c2jm30804e

broken down with sonication to obtain nanoporous ormosil colloids.

The nanoporous ormosil colloids can be deposited on almost any surface with spin, dip or spray coating methods. In this study we prepared several AR ormosil thin films on glass and cellulose acetate (CA) substrates. The stability of the films was demonstrated by water dripping tests. We observed that the films are durable even after 90 h of water dripping. Furthermore, the films remain on the substrate after adhesive tape tests, indicating strong adhesion between the substrate and the ormosil films. Ormosil thin films prepared on CA substrates preserve their AR properties even after 100 cycles of bending (bending radius is 2.5 mm). The significant flexibility and durability of the ormosil coatings is due to their hybrid nature. In ormosils, organic groups which are covalently bonded to a durable silica network provide flexibility by decreasing crosslinking.[25] In addition, we tuned the porosity (therefore the refractive index) of the films by simply changing the ratio of the monomers in the starting solution. Furthermore, superhydrophilicity can be added to the thin films by annealing. The annealed superhydrophilic AR thin films prevent the formation of fog (antifogging) by spreading the condensed water onto the surface, forming a thin water film and thus preserving the transparency. We successfully prepared AR and antifogging coatings on glass substrates by annealing the ormosil thin films at 600 °C.

Experimental

MTMS, TEOS, methanol, oxalic acid, and ammonium hydroxide (26%) were purchased from Sigma-Aldrich (U.S.) and used as purchased. Gels were obtained by slightly modifying a previously reported two-step sol–gel method.[26] In the first step, x mL ($0 \leq x \leq 1$) of TEOS and $1–x$ mL of MTMS were dissolved in 9.74 mL of methanol. Following the addition of 0.5 mL of 0.01 M aqueous oxalic acid solution the reaction mixture was stirred for 30 min and left for hydrolysis for 24 h at room temperature. After the hydrolysis, 0.40 mL of ammonium hydroxide (26%) and 0.21 mL of water were added dropwise to the reaction mixture in order to catalyze the condensation reaction. Following 15 min of stirring, the solution was left for gelation and aged for 2 days at room temperature after gelation. 15 mL of methanol was added to the resulting gel and sonicated using an ultrasonic liquid homogenizer[27] for 45 to 75 s at 20 W power. The obtained colloidal suspensions were spin coated at a rate of 2000 rpm on surfaces which were cleaned by sonication in ethanol for 15 min. For the complete evaporation of the remaining solvent, the prepared ormosil films were left to dry at room temperature overnight or for 15 min in a vacuum oven at 50 °C. The films were named with the number in the abbreviation indicating the TEOS volume fraction, such that T40 indicates the film containing 40% TEOS and 60% MTMS.

Microstructural observations of the thin films were carried out using an environmental scanning electron microscope and a scanning electron microscope (E-SEM, Quanta 200F, FEI and NanoSEM, Nova, FEI on ultra-high resolution mode with a Helix detector) at low vacuum conditions. The skeletal and porous structure of the ormosil colloids were visualized by bright-field images with a transmission electron microscope (TEM, Tecnai G2 F30, FEI) operated at 200 kV. The TEM

samples were prepared on a holey carbon coated copper grid by placing a drop of the colloidal suspension used for film production. The surface roughness of the films prepared on glass substrates was analyzed using an atomic force microscope (AFM, XE-100E, PSIA) in non-contact mode. Thickness and spectroscopic refractive index measurements were obtained by an Ellipsometer (V-Vase, J. A. Woollam) using the Cauchy model ($n(\lambda) = A + B/\lambda^2 + C/\lambda^4$). The Cauchy model is selected since the ormosil films are transparent, i.e. $k(\lambda) = 0$, in the experimental range (400 to 1000 nm). Optical transmission measurements were carried out using a UV-vis spectrophotometer (Cary 100, Varian). A contact angle meter (OCA 30, Dataphysics) was used to measure the static water contact angles on the ormosil thin films before and after annealing steps. Water droplets of 4 μL volume were used with Laplace–Young fitting for contact angle measurements. Chemical analysis of the surface was performed using X-ray photoelectron spectroscopy (XPS, K-Alpha, Thermo Scientific).
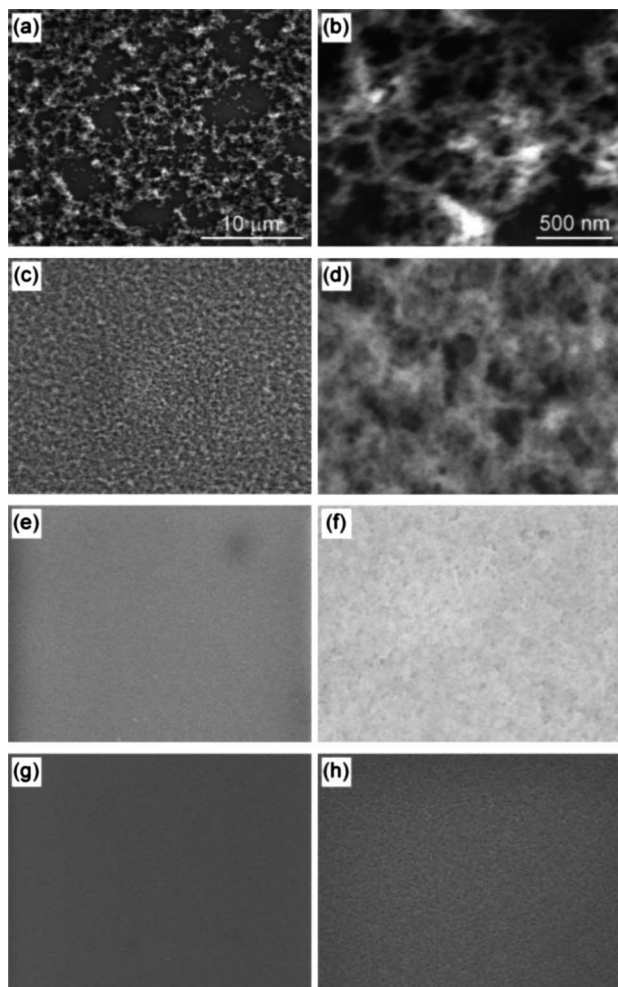
Results and discussion

Porous ormosil thin films with thickness values around 100 nm are produced from colloidal suspensions which are prepared by the sonication of ormosil gels. We prepared several ormosil gels by using different volume ratios of TEOS and MTMS monomers in the starting solution. The gels prepared using only MTMS monomer are opaque due to macroscopic phase separation during gelation, induced by cyclic and cage-like closed species formed during polymerization of the MTMS monomer. The porous ormosil thin films obtained from these phase separated gels show superhydrophobic behavior,[22] because of their dual scale (micrometer and nanometer sized structures) roughness and methyl groups covering the surface. The surface methyl groups also prevent pore collapse during solvent evaporation (spring-back effect) under ambient conditions and result in a highly porous structure.[20,26–28] However, the thin films prepared from such macroscopic phase separated MTMS based gels have a slightly translucent appearance and for the films with thicknesses lower than 500 nm non-uniform film formation is observed.[22,23] In order to prepare very thin and uniform films, phase separation in the MTMS based gels must be prevented. It is known that some additional monomers,[24] surfactants[19] or polar solvents[17] can prevent phase separation. In this study we used TEOS monomer to prevent the phase separation in MTMS based gels. We observed that, addition of TEOS monomer increased the transparency (and thus homogeneity) of the gels and after a 40% v/v TEOS ratio, completely transparent and homogenous gels were obtained. By using these homogenous gels, we prepared several uniform and nanoporous ormosil thin films.
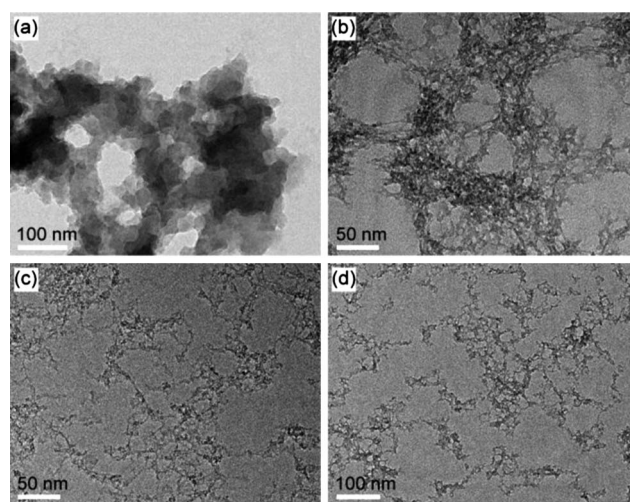
The surface morphology of the thin films was characterized by SEM (Fig. 1). It can be seen that as the TEOS fraction increases, the micrometer sized pores start to disappear and more uniform films are formed. The T0 film (Fig. 1a and b) has poor surface coverage with uncoated regions. On the other hand, starting from the T25 film (Fig. 1c and d), uniform films were obtained without micrometer sized pores, which indicate that the addition of the TEOS monomer provides uniform film formation. It was also seen from higher magnification SEM images that as the

TEOS ratio increases the pore sizes decrease. T60 (Fig. 1e and f) has smaller pores than T25, whereas T80 (Fig. 1g and h) has even smaller pores than the T60 film. However, the T100 film shrank and cracked during drying due to its hydrophilic and rigid nature (Fig. S1, ESI†). On the other hand, films containing the MTMS monomer provide spring-back as a result of the hydrophobic methyl groups which decrease capillary tension in addition to providing flexibility. Thus, an optimum fraction of MTMS should be used for obtaining a flexible and uniform film. The pore sizes and skeletal structures of the T0, T25, T60 and T80 films are identified in detail using TEM (Fig. 2). The skeletal structure of the T0 film is composed of cross linked tens of nanometer sized ormosil clusters which are surrounded by nanometer sized pores (Fig. 2a). As the TEOS ratio increases, the domain sizes of interconnected clusters decrease and the pores surrounding these domains become smaller, which helps to improve the homogeneity of the obtained films. T80 has the thinnest skeletal structure and the smallest pores, as can be seen in Fig. 2d.

The surface topography of the prepared T0, T25, T60 and T80 films was investigated using the AFM technique in non-contact

Fig. 2 TEM micrographs of (a) T0, (b) T25, (c) T60 and (d) T80 films, showing the skeletal structure of the ormosil films. As the TEOS fraction increases, interconnected branches get thinner.

mode (Fig. 3). The results obtained from AFM are in accordance with the SEM and TEM results, indicating that the films prepared from the TEOS/MTMS hybrid gels result in better surface coverage and a more uniform structure. While there are uncoated regions and high height differences between the domains for the T0 film, with increasing TEOS fraction, the surface is covered better with similar sized ormosil clusters. Low surface roughness is crucial for AR surfaces because a surface roughness higher than 50 nm results in the scattering of incident light from the surface. The average roughness values of the films are determined on the basis of the AFM measurements obtained from 3 different $10 \times 10\ \mu m^2$ regions of each film. A plot of the average surface roughness *vs.* TEOS fraction clearly shows that the average surface roughness drastically decreases from 122 nm
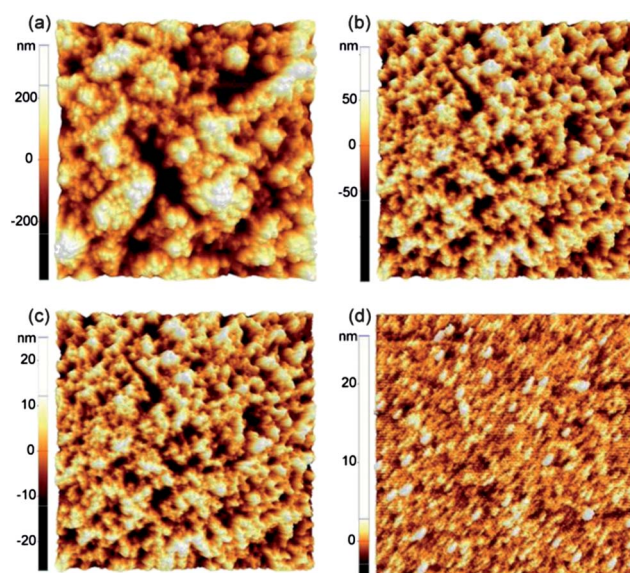

Fig. 1 SEM micrographs of (a,b) T0, (c,d) T25, (e,f) T60 and (g,h) T80 films, which indicate that the surface coverage and uniformity of the ormosil films improve with increasing amount of TEOS, in addition to decreasing pore sizes.

Fig. 3 AFM images of (a) T0, (b) T25, (c) T60 and (d) T80 films taken from a $10 \times 10\ \mu m^2$ area, showing that as the TEOS fraction increases, the average roughness and cluster size decrease.
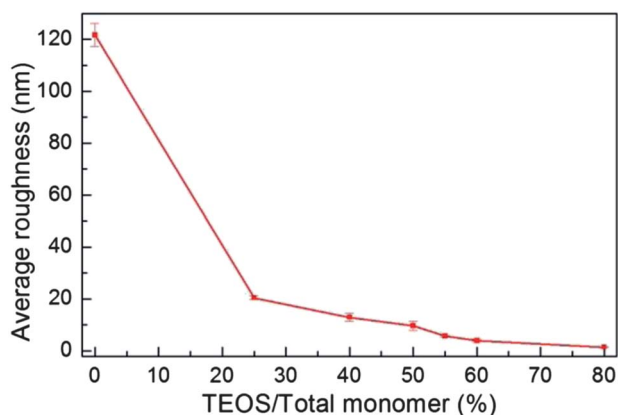
Fig. 4 Average surface roughness as a function of the TEOS fraction graph, indicating that as the TEOS ratio increases, the average surface roughness decreases. Even 25% TEOS addition causes around a 100 nm decrease in the average roughness.
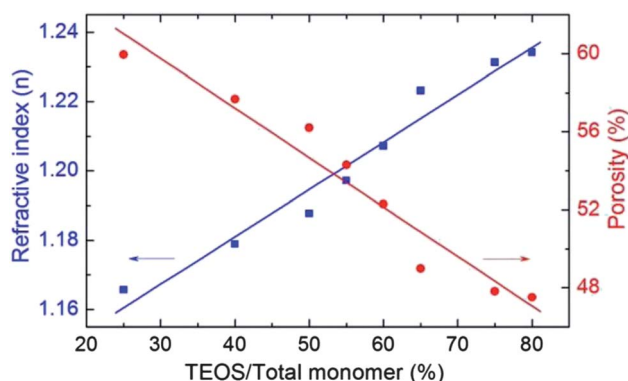
Fig. 5 Effect of the TEOS fraction on the refractive index and percent porosity. As the TEOS fraction increases, the refractive index increases due to decreasing porosity. This dependence of refractive index on the TEOS fraction enables the preparation of thin films with different refractive indexes which can be used with different substrates.
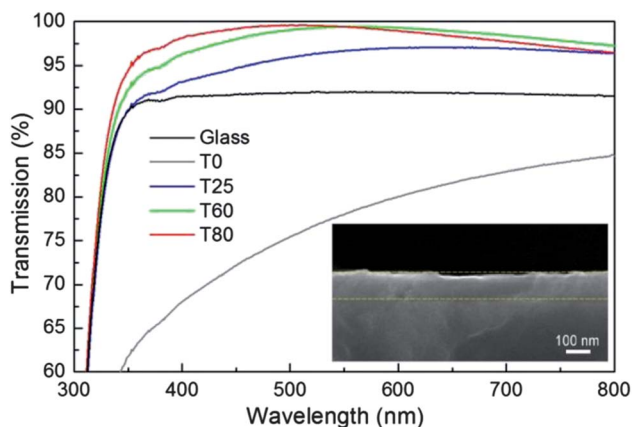

Fig. 6 Transmission spectra of double side coated substrates with T0, T25, T60 and T80 films and a bare glass slide. The MTMS-TEOS hybrid films exhibit AR properties on the glass substrate with the transmission reaching 99.5%. The inset shows a cross sectional SEM image of the T60 film, indicating the homogeneity in thickness.
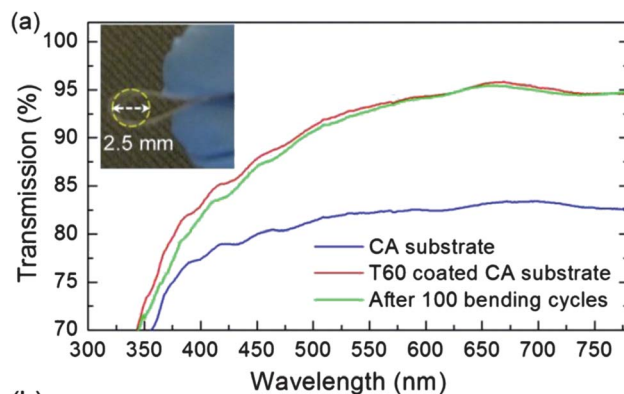

Fig. 7 (a) Transmission spectra of uncoated CA substrate (blue), T60 coated (both sides) CA substrate before (red) and after (green) 100 cycles of excessive bending, showing that the T60 films are also flexible in addition to being AR. A photograph of the bent CA substrate is given as the inset, indicating the bending radius of 2.5 mm. (b) Photograph showing T60 coated (left) and bare CA substrates (right). Whereas the coated substrate exhibits AR properties, the uncoated substrate reflects ambient daylight.

to a few nanometers with increasing TEOS fraction (Fig. 4). For T25, the average roughness decreases to 24 nm, and for T80 it becomes 1.45 nm. For films with such low roughness, light scattering due to surface roughness can be ignored.

The refractive indices of the ormosil films was measured using spectroscopic ellipsometry in reflection mode and porosities of the films were calculated from the refractive index–porosity equation, *i.e.* by comparing the porous films with nonporous reference thin films.[23,28] The index of refraction and the percent porosity *vs.* the TEOS fraction graph is given in Fig. 5. The index of refraction of these ormosil films varies in the range of 1.23 to 1.17, depending on the TEOS fraction, and the percent porosity varies between 60 and 48%. It can be seen that the index of refraction values change almost linearly, depending on the TEOS fraction. As the TEOS fraction increases, the porous gel structure becomes more hydrophilic because of the hydroxyl groups of not fully condensed TEOS monomers. As a result of the more hydrophilic surface, the pores of higher TEOS containing films have higher tendency to collapse during solvent evaporation, thus the porosity of these films decreases. The T100 film does not contain any hydrophobic moieties to provide a spring-back effect. As a result, the capillary tension existing during solvent evaporation shrunk the pores and thus, a cracked and dense film was formed. However, even at very low MTMS concentrations, the films revealed significant porosity (48% for T80), which
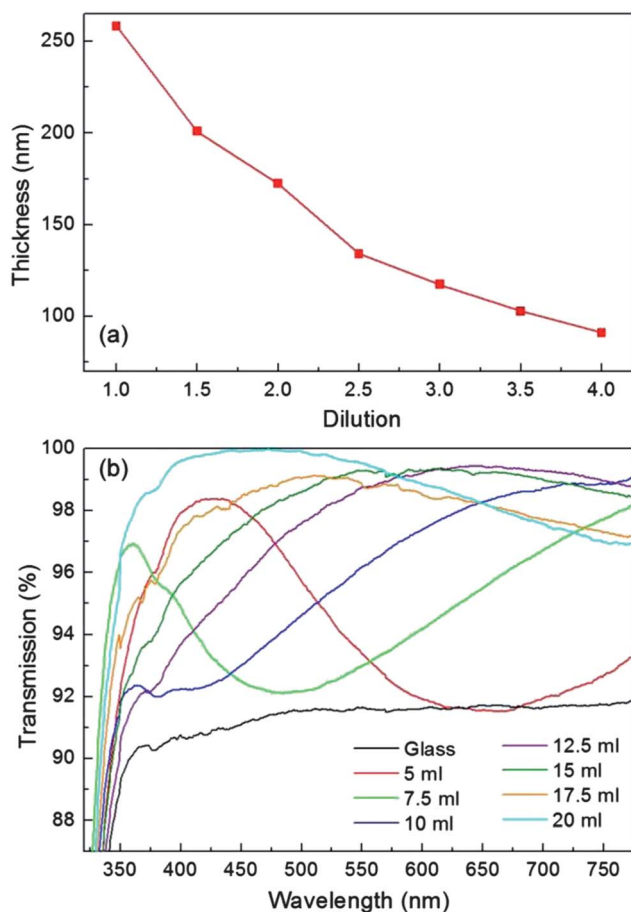
Fig. 8 (a) Effect of dilution of the suspension on the thickness of T60 film, indicating that the thickness can be controlled by dilution in the range of 260–90 nm. (b) The transmission of T60 film for different thicknesses. As the film gets thinner, the transmission maximum shifts to lower wavelengths.
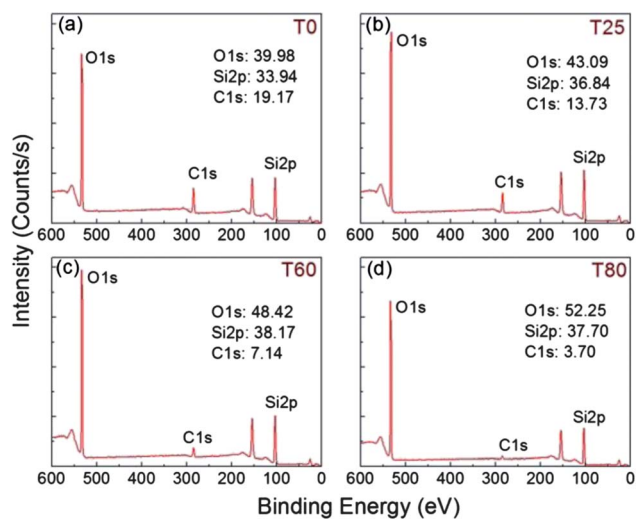
Fig. 9 XPS results of (a) T0, (b) T25, (c) T60 and (d) T80 films, indicating that as the TEOS ratio increases the relative ratio of C atoms decreases, whereas the O atoms increase.
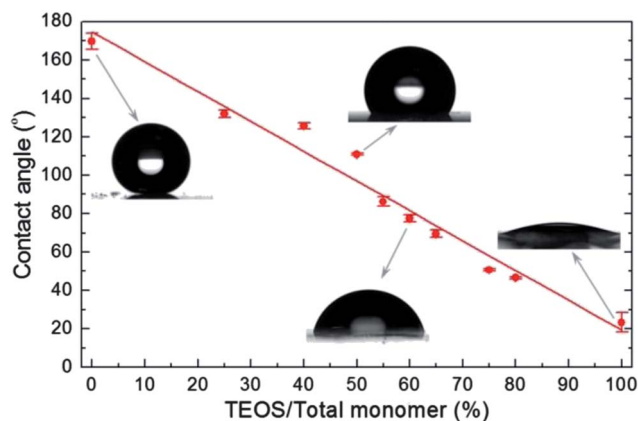

Fig. 10 Change of contact angle with respect to the TEOS fraction, showing that as the TEOS fraction increases the surface becomes more hydrophilic. Inset: photographs of T0, T40, T60 and T100 films are used to visualise how water droplets spread on each surface, respectively.

proves that small fractions of the surface methyl groups can provide the spring-back effect.

Enhanced light transmission from double side coated substrates with different ormosil thin films are shown in Fig. 6. In order to get transmission maxima in the visible spectrum, the thickness of the films was adjusted to around 125 nm by diluting the colloids (will be discussed in detail), which were measured by spectroscopic ellipsometry. All of the hybrid thin films enhance the light transmission of the glass substrate due to their low refractive indices and surface roughness values. For T80 film, light transmission reaches 99.58% at 510 nm. Also, T60 ormosil film exhibited a very high transmission maximum which is 99.43% at 550 nm. However, the films prepared from pure MTMS or TEOS monomers (data not shown) decrease the transmission because of their high surface roughnesses. A cross-sectional SEM image of T60 film with a thickness of ~100 nm on a silicon substrate is given in the inset of Fig. 6 (additional SEM micrographs of T60 and T75 are given in Fig. S2†) which shows the uniformity of the coating.

The mechanical stability of the hybrid films was tested by water dripping[29,30] scratching[31,32] (ASTM D3363 standard) and adhesive tape tests.[33,34] In the water dripping test, films on glass substrates, placed with an inclination of 45°, were treated by water droplets (~100 μL) falling from 30 cm at a rate of one drop per second. After 24 h of the water dripping test (~86 400 droplets) the surfaces of all films (T0, T25, T60 and T80) remained antireflective with slight decreases in transmission (Fig. S3, ESI†). T60 film is further tested for up to 90 h of water dripping (324 000 droplets), which resulted in only a 0.9% decrease in transmission. The SEM micrographs of T60 taken after 90 h of the water dripping test revealed that the nanoporous and homogeneous structure of the film is not affected by the test (Fig. S4, ESI†). These results indicate that the films are stable against excessive water dripping. The films were scratched with a series of pencils of different hardnesses (between 6H to 8B) by applying approximately 1 MPa of pressure. After the scratch test, the surface morphologies were investigated by SEM, which indicated that most of the coating was removed upon scratching. The SEM images also revealed that as the hardness decreased,
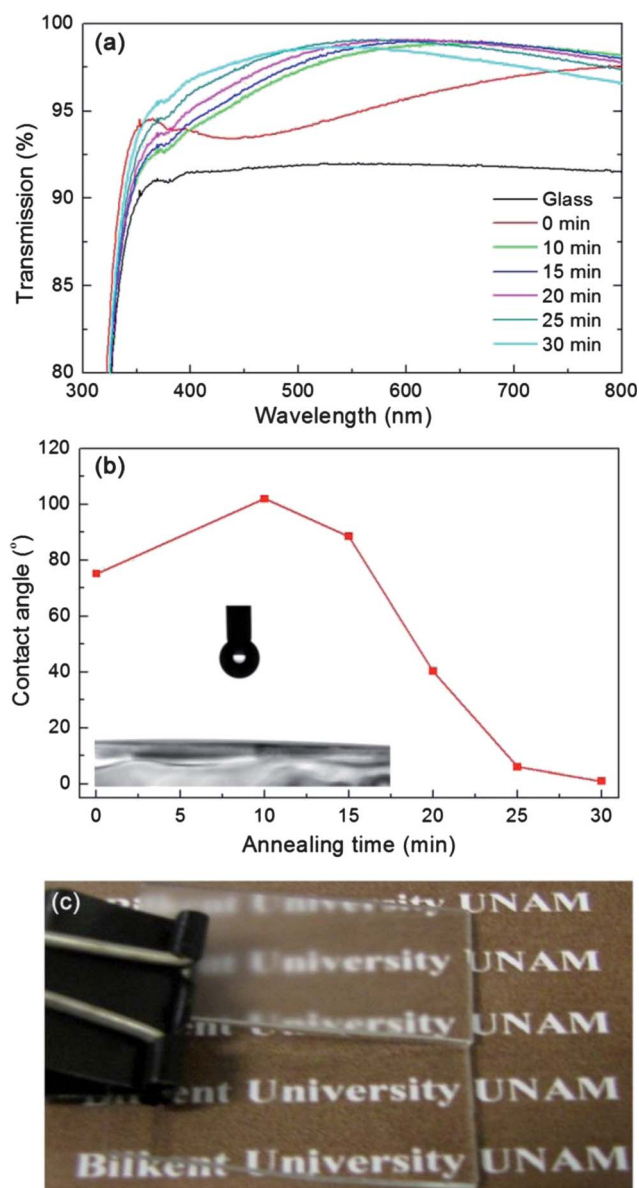
Fig. 11 (a) Effect of annealing at a temperature of 600 °C for different durations on the transmission for T60 film. (b) The change in contact angle as a function of annealing time for T60 film at 600 °C. Film becomes more hydrophobic following an annealing of 10 min, but after 30 min the film becomes superhydrophilic. Inset: a photograph taken during contact angle measurement showing that after 30 min annealing at 600 °C the film becomes superhydrophilic with a contact angle reaching 0°. (c) A photograph visualizing the antifogging properties of 30 min annealed T60 film. While there is no fog formation for the coated glass (lower slide), there is fog on the uncoated glass (upper slide), following the recovery of cooled slides from −20 °C to room temperature.

the amount of removed material from the films decreased (Fig. S5, ESI†). Furthermore, for T60 and T80 films no removal was observed when the softest pencil (8B) was used. The low resistance of the ormosil coatings against mechanical scratching is due to their porosity and ultralow thickness. Furthermore, adhesion of T60 film on glass substrates was tested using scotch tape. The surfaces were pressed with adhesive tapes applying approximately 10 kPa of pressure. When peeling the tape from

the ormosil film, some of the adhesive material of the tape remains on the film. This indicates that adhesion between the ormosil film and the substrate is stronger than adhesion between the adhesive layer and the tape substrate.

The ormosil coatings are expected to be flexible because of the covalently bonded organic moieties on the silica network even though the fraction of the MTMS monomer is low.[35] To test the flexibility of the ormosil films, we prepared T0, T25, T60 and T80 films on CA substrates. In Fig. 7a, the bending test results for T60 are given. The uncoated substrate has around 80% transmission, whereas the double side coated substrate has around 95% transmission at 600 nm. T60 film was found to preserve its AR properties even after 100 cycles of excessive bending (bending radius is 2.5 mm), which proves that the coating is deformable. For bending radii smaller than 2.5 mm the substrate starts to deform plastically. A photograph showing the bending of T60 film on CA substrate is given in Fig. 7a as inset. Similar results were also obtained for T0, T25 and T80 films (Fig. S6, ESI†). Also the AR property of the T60 ormosil coating is visualized on the T60 coated and uncoated CA substrates (Fig. 7b). As can be seen, there is high reflection on the uncoated substrate (right), whereas there is negligible reflection on the coated substrate (left).

The wavelength of the transmission maximum can be tuned by changing the film thickness. In order to tune the film thickness we diluted a concentrated ormosil colloidal suspension (prepared by a 5 mL methanol addition to the gel) with methanol. The suspension was diluted with 2.5 mL portions of methanol until it reached a total dilution volume of 20 mL methanol and following every addition, the suspension was sonicated for 5 s. The film thickness decreases almost linearly after every dilution (Fig. 8a). As can be seen from Fig. 8b, for all dilution ratios, the films exhibit AR property, and as the dilution increases, the point of maximum transmission shifts to lower wavelengths. The thickness of the 5 mL diluted film was ellipsometrically measured to be 260 nm and the thickness of the 20 mL diluted film decreases to 90 nm.

XPS analysis was performed in order to investigate the chemical composition of the ormosil surfaces. Relative ratios of only silicon, oxygen and carbon atoms for the T0, T25, T60 and T80 films (Fig. 9) are taken into consideration. As the TEOS ratio increases, the relative ratio of O atoms gradually increased from 39.98 to 52.25% and the relative ratio of C atoms gradually decreased from 19.17 to 3.70%. This stems from the replacement of the nonhydrolyzable methyl group containing MTMS with TEOS.

The wetting properties of the hybrid films were investigated with a contact angle meter system. The water contact angles of the films also linearly changed with respect to the TEOS fraction (Fig. 10). T0 film was found to be superhydrophobic with a water contact angle of 178.4°, and T100 film was found to be hydrophilic with a contact angle of 23.3°. On the other hand, the hybrid films exhibited contact angles ranging from 140° to 40°. As the fraction of MTMS decreases, the films tend to become more hydrophilic because the hydrophobicity arises as a result of the methyl groups of MTMS. In addition to the absence of methyl groups, the decrease in the surface roughness also affects the water contact angles.

T60 film coated on glass substrate was annealed at 600 °C for 30 min in order to make it superhydrophilic.[22,36] During

9676 | *J. Mater. Chem.*, 2012, **22**, 9671–9677

This journal is © The Royal Society of Chemistry 2012

annealing, the thickness of the film gradually decreases because of the material loss at high temperatures. In order to obtain a superhydrophilic and AR coating at visible wavelengths, we first prepared a T60 film with a thickness around 200 nm which gives a transmission maximum in the infrared region. During annealing, the transmission maximum of the film shifted to smaller wavelengths because of the decrease in the film thickness (Fig. 11a). After annealing for 30 min, the transmission maximum reaches 550 nm, which correspond to a thickness around 135 nm. The dependence of the contact angle of the T60 film on the annealing duration is shown in Fig. 11b. The contact angle first increases a little due to the removal of some unreacted species,[17] then starts to decrease due to the replacement of methyl groups with hydroxyls. Finally, the surface becomes superhydrophilic with the contact angle reaching 0° (Fig. 11b, inset). In order to show the antifogging properties, a fogging test was performed by placing 30 min annealed T60 film and an uncoated glass substrate into a freezer at −20 °C for 5 min. Following removal from the freezer, a fog layer spontaneously forms on the uncoated substrate, while it does not form on the coated substrate (Fig. 11c). These antifogging properties stem from the spreading of water on the superhydrophilic surface, forming a uniform water layer on the surface, whereas on the plain glass, water droplets form islands, causing the scattering of light.

Conclusions

In conclusion, we prepared flexible AR coatings from ormosil colloids which are prepared using MTMS and TEOS based hybrid gels. We observed that the MTMS monomer provides flexibility and porosity to the coatings; on the other hand, the TEOS monomer provides transparency, thickness uniformity and a smooth surface, while decreasing the porosity. The porosity of these hybrid ormosil coatings can be tuned by simply changing the monomer ratio, and the thickness of the coatings can be controlled by adjusting the colloid concentration. The nanoporous and uniform ormosil coatings reveal AR properties on glass and CA substrates. The AR films on flexible CA substrates retain their AR properties even after 100 cycles of excessive bending without a significant change in transmission. It is shown that the films on glass substrates are stable against excessive water dripping and there is strong adhesion between the films and substrates. In addition, AR coatings on glass substrates exhibit antifogging properties after annealing at 600 °C. This facile and low-cost fabrication method of flexible and mechanically stable AR and antifogging coatings makes them suitable for several application fields including solar cells, flexible electronics, and optical devices.

Acknowledgements

References

1 L. Zhang, Z. A. Qiao, M. Zheng, Q. Huo and J. Sun, *J. Mater. Chem.*, 2010, **20**, 6125.
2 M. Faustini, L. Nicole, C. Boissiere, P. Innocenzi, C. Sanchez and D. Grosso, *Chem. Mater.*, 2010, **22**, 4406.
3 H. Yabu and M. Shimomura, *Chem. Mater.*, 2005, **17**, 5231.
4 X. Li, J. P. Gao, L. J. Xue and Y. C. Han, *Adv. Funct. Mater.*, 2010, **20**, 259.
5 R. G. Karunakaran, C. H. Lu, Z. H. Zhang and S. Yang, *Langmuir*, 2011, **27**, 4594.
6 A. L. Penard, T. Gacoin and J. P. Boilot, *Acc. Chem. Res.*, 2007, **40**, 895.
7 P. Nostell, A. Roos and B. Karlsson, *Thin Solid Films*, 1999, **351**, 170.
8 W. Shimizu and Y. Murakami, *ACS Appl. Mater. Interfaces*, 2010, **2**, 3128.
9 Z. Wu, J. Walish, A. Nolte, L. Zhai, R. E. Cohen and M. F. Rubner, *Adv. Mater.*, 2006, **18**, 2699.
10 M. Manca, A. Cannavale, L. De Marco, A. S. Arico, R. Cingolani and G. Gigli, *Langmuir*, 2009, **25**, 6357.
11 H. Y. Koo, D. K. Yi, S. J. Yoo and D. Y. Kim, *Adv. Mater.*, 2004, **16**, 274.
12 J. Xiong, S. N. Das, B. Shin, J. P. Kar, J. H. Choi and J. M. Myoung, *J. Colloid Interface Sci.*, 2010, **350**, 344.
13 P. Podsiadlo, L. Sui, Y. Elkasabi, P. Burgardt, J. Lee, A. Miryala, W. Kusumaatmaja, M. R. Carman, M. Shtein, J. Kieffer, J. Lahann and N. A. Kotov, *Langmuir*, 2007, **23**, 7901.
14 S. Walheim, E. Schaffer, J. Mlynek and U. Steiner, *Science*, 1999, **283**, 520.
15 J. Hiller, J. D. Mendelsohn and M. F. Rubner, *Nat. Mater.*, 2002, **1**, 59.
16 J. C. Hsu, P. W. Wang, Y. H. Lin, H. L. Chen, Y. Y. Chen, Y. D. Yao and J. C. Yu, *Opt. Rev.*, 2010, **17**, 553.
17 A. Yildirim, H. Budunoglu, M. Yaman, M. O. Guler and M. Bayindir, *J. Mater. Chem.*, 2011, **21**, 14830.
18 S. R. Forrest, *Nature*, 2004, **428**, 911.
19 K. Kanamori, M. Aizawa, K. Nakanishi and T. Hanada, *Adv. Mater.*, 2007, **19**, 1589.
20 A. V. Rao, S. D. Bhagat, H. Hirashima and G. M. Pajonk, *J. Colloid Interface Sci.*, 2006, **300**, 279.
21 H. Dong, R. F. Reidy and J. D. Brennan, *Chem. Mater.*, 2005, **17**, 6012.
22 H. Budunoglu, A. Yildirim, M. O. Guler and M. Bayindir, *ACS Appl. Mater. Interfaces*, 2011, **3**, 539.
23 A. Yildirim, H. Budunoglu, H. Deniz, M. O. Guler and M. Bayindir, *ACS Appl. Mater. Interfaces*, 2010, **2**, 2892.
24 L. Martin, J. O. Osso, S. Ricart, A. Roig, O. Garcia and R. Sastre, *J. Mater. Chem.*, 2008, **18**, 207.
25 H. S. Lim, J. H. Baek, K. Park, H. S. Shin, J. Kim and J. H. Cho, *Adv. Mater.*, 2010, **22**, 2138.
26 S. D. Bhagat, C. S. Oh, Y. H. Kim, Y. S. Ahn and J. G. Yeo, *Microporous Mesoporous Mater.*, 2007, **100**, 350.
27 S. S. Prakash, C. J. Brinker, A. J. Hurd and S. M. Rao, *Nature*, 1995, **374**, 439.
28 G. S. Kim and S. H. Hyun, *Thin Solid Films*, 2004, **460**, 190.
29 Y. Li, F. Liu and J. Sun, *Chem. Commun.*, 2009, 2730.
30 A. Yildirim, H. Budunoglu, B. Daglar, H. Deniz and M. Bayindir, *ACS Appl. Mater. Interfaces*, 2011, **3**, 1804.
31 D. K. Hwang, J. H. Moon and Y. G. Shul, *J. Sol-Gel Sci. Technol.*, 2003, **26**, 783.
32 Z. Chen, L. Y. L. Wu, E. Chwa and O. Tham, *Mater. Sci. Eng., A*, 2008, **493**, 292.
33 X. Deng, L. Mammen, Y. Zhao, P. Lellig, K. Mullen, C. Li, H. J. Butt and D. Vollmer, *Adv. Mater.*, 2011, **23**, 2962.
34 H. Jiang, W. Zhao, C. Li and Y. Wang, *Soft Matter*, 2011, **7**, 2817.
35 G. Palmisano, E. Le Bourhis, R. Ciriminna, D. Tranchida and M. Pagliaro, *Langmuir*, 2006, **22**, 11158.
36 N. J. Shirtcliffe, G. McHale, M. I. Newton, C. C. Perry and P. Roach, *Chem. Commun.*, 2005, 3135.